Proceedings of the ASME 2010 Pressure Vessels & Piping Division / K-PVP Conference
PVP2010
July 18-22, 2010, Bellevue, Washington, USA

PVP2010-25696

MULTIPHASE FLUID STRUCTURE INTERACTION IN BENDS AND T-JOINTS

Marcos F. Cargnelutti
TNO Science and Industry
Delft, The Netherlands

Stefan P.C. Belfroid
TNO Science and Industry
Delft, The Netherlands

Wouter Schiferli
TNO Science and Industry
Delft, The Netherlands

Marlies van Osch
TNO Science and Industry
Delft, The Netherlands

ABSTRACT

Air-water experiments were carried out in a horizontal 1" pipe system to measure the magnitude of the forces induced by the multiphase flow. Forces and accelerations were measured on a number of bends and T-joint configurations for a wide range of operating conditions. Five different configurations were measured: a baseline case consisting of straight pipe only, a sharp edged bend, a large radius bend, a symmetric T-joint and a T-joint with one of the arms closed off.
The gas flow was varied from a superficial velocity of 0.1 to 30 m/s and the liquid flow was varied from 0.05 to 2 m/s. This operating range ensures that the experiment encompasses all possible flow regimes.

In general, the slug velocity and frequency presented a reasonable agreement with classical models. However, for high mixture velocity the measured frequency deviated from literature models.

The magnitude of the measured forces was found to vary over a wide range depending on the flow regime. For slug flow conditions very high force levels were measured, up to 4 orders of magnitude higher than in single phase flow for comparable velocities. The annular flow regime resulted in the (relative) lowest forces, although the absolute amplitude is of the same order as in the case of slug flow. These results from a one inch pipe were compared to data obtained previously from similar experiments on a 6mm setup, to evaluate the scaling effects. The results for the one inch rig experiments agreed with the model proposed by Riverin, with the same scaling factor. A modification of this scaling factor is needed for the model to predict the forces measured on the 6mm rig.

The validity of the theories developed based on the 6mm experiments were tested for validity at larger scales. In case of slug flow, the measured results can be described assuming a simple slug unit model. In annular and stratified flow a different model is required, since no slug unit is present. Instead, excitation force can be estimated using mixture properties. This mixture approach also describes the forces for the slug regime relatively well. Only the single phase flow is not described properly with this mixture model, as would be expected.

INTRODUCTION.

Flow assurance is often taken to include mostly events occurring inside a flowline or well, such as wax deposition or the formation of hydrates. However, structural integrity of a piping system is obviously a basic requirement for flow assurance. This can become an issue in many situations. In single phase flow, waterhammer waves caused by fast valve closures may cause high loads. In multiphase flows these problems may be exacerbated: in slug flow, for example, slugs of water move at high velocities dictated by the gas flow, resulting in high momentum and consequently high forces in locations where the flow change direction.

The goal of this work is to determine the amplitude and frequency response of the dynamic forces on bend structures for a large range of operating conditions and regimes. In this paper five different geometries are analysed. A single straight pipe, two different bends, one T-joint and one T-joint in which one of the legs was closed off, forming a sharp bend. Little experimental data is available of actual measurements on similar systems. The forces induced on a bend by a multiphase flow mixture were investigated previously by Riverin et al. [1] and Tay and Thorpe [2], among others. The authors have published some materials on a 6mm scale [3].

NOMENCLATURE

A	Tube cross sectional area	[m^2]
C	Force proportionally factor	[-]
C_o	Distribution parameter	[-]
D	Tube diameter	[m]
F_{rFet}	Fetter slug frequency Froude number	[-]
F_{rg}	Froude gas number	[-]
F_{rl}	Froude liquid number	[-]
F_{rms}	RMS value of F_R	[N]
F_{std}	Standard deviation of F_R	[N]
Re_m	Mixture Reynolds number	[-]
Sr	Strouhal number	[-]
We	Weber number	[-]
f_{slug}	Slug frequency	[Hz]
g	Gravitational acceleration	[m/s^2]
l_{slug}	Liquid slug length	[m]
u_m	Mixture velocity	[m/s]
$u_{s,g}$	Superficial gas velocity	[m/s]
$u_{s,l}$	Superficial liquid velocity	[m/s]
u_{slug}	Slug velocity	[m/s]
α_l	Liquid hold-up	[-]
η_l	Liquid viscosity	[Pa s]
η_l	Liquid density	[kg/m^3]
σ	Surface tension	[N/m]

EXPERIMENTAL SETUP

The experimental setup consists of a perspex pipe with a length of 2600mm and an internal diameter of one inch (254 mm). The air is provided by a central compression system. The liquid used is ultra pure water. The maximum (superficial) flow velocity for the gas is u_{sg}=70 m/s and for the liquid u_{sl}=3 m/s. The mixing of the two fluids occurs in a y-piece (Figure 1), with the air coming from above. The outlet is a large separator vessel. The pipes (straight pipe, bends or Tjoint) are attached to the separator using a flexible hose.

Figure 1: Water-air mixing point.

Figure 2 presents a schematic distribution of the test rig, showing the location of the pressure, force and optical sensors. Typically, four dynamic pressure transducers (Kulite XCE-093, HBM P3MB) were used to measure pressure fluctuations. Three of these were placed upstream of the bend, to determine the pressure drop and in particular the slug characteristics such as frequency and velocity. The fourth sensor was placed downstream of the bend and was used to calculate the pressure drop across the bend. Two force sensors (B&K 8302 sn: 10187) were situated at the bend. One upstream and one downstream, both perpendicular to the tube.

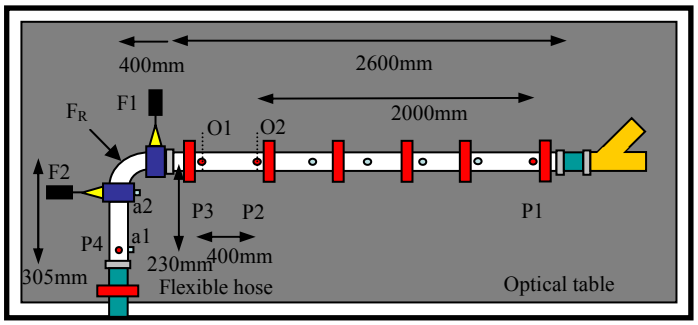

Figure 2: Schematic of the experimental setup.

Figure 3 presents the location of the force sensors for both the bend and the t-join experiments. The force sensors were zeroed at no-flow conditions. Optical sensors (Thorlabs Inc. PPDA/LSD1) were used to detect whether liquid or gas was present in the tube. These were simple light emitters and light sensors which allowed for detection of slugs. However, high gas content slugs proved to be difficult to measure. Finally, a high speed camera (DEWE-CAM-01) was used to film the flow approaching the bend. All measurements were recorded using a Dewetron data acquisition system. This allowed for direct simultaneous recording of all signals including the camera.

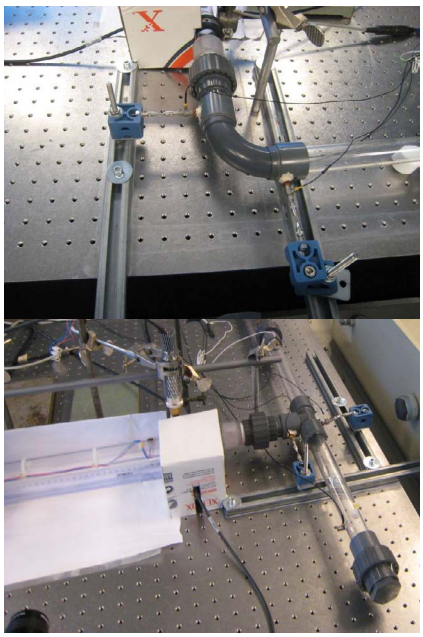

Figure 3: Setup of force transducers.

Five geometries were tested: a single straight pipe, two different bends (named Bend1 and Bend2), one T-joint and one T-joint in which one of the legs was closed off (named T-bend)

(Figure 4). The leg was closed off with a leg remaining of 345mm.

In the experiments the measured force was affected by the mechanical response of the complete system, consisting of the tube and the support clamps. The supports were positioned sufficiently far from the bend, that no effect on the forces could be measured. Using a Teflon block to support the bend in the tubing allowed for relatively free movement in the horizontal plane while limiting vertical displacement. In the results of the force measurements, a resulting force F_R (see Figure 2) is presented. This force, for the bend experiments (Bend1, Bend2 and T-bend), is given by:

$$F_R = \sqrt{F_1^2 + F_2^2} \tag{1}$$

For the T-joint this resulting force is given by:

$$F_R = \sqrt{F_1^2} \tag{2}$$

Figure 4: Three test geometries (Top left: Bend1, Top right: Bend2, bottom T-Joint).

EXPERIMENTAL RESULTS

Flow characteristics – flow map

In Figure 5 the experimental flow regime map is compared to the classic flowmaps of Mandhane and Baker [4], [5]. Mandhane's flow map is based on pipe diameters ranging from 12.7 mm to 165.1 mm. The Baker flowmap is also based on a large number of experiments. The flowmap derived from the visual observations in these experiments shows good agreement with the classical flowmaps. This is a good indication that the inflow length of this set-up is sufficiently long to produce fully developed slug flow.

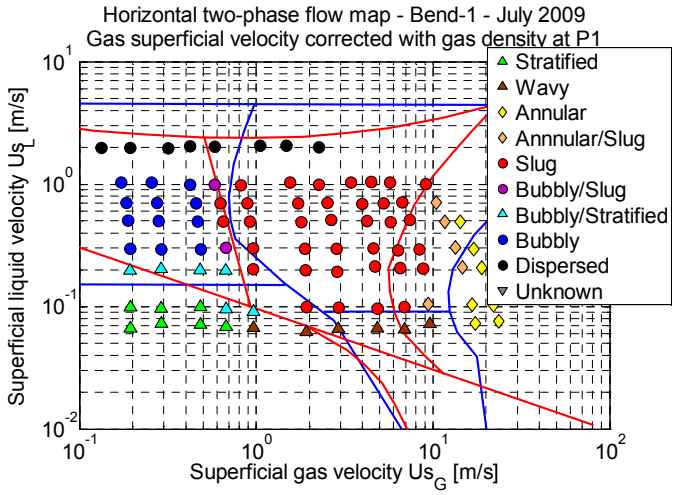

Figure 5: Flow regime map based on visual observations. The red lines indicate the classic flowmap according to Baker [5], the blue lines indicate the flowmap according to Mandhane [4].

Flow characteristics – slug flow

Force and pressure fluctuations in the slug regime are expected to be affected by slug flow characteristics such as slug velocity, slug frequency and slug length. The slug characteristics are calculated from the optical sensor data and the pressure signals.

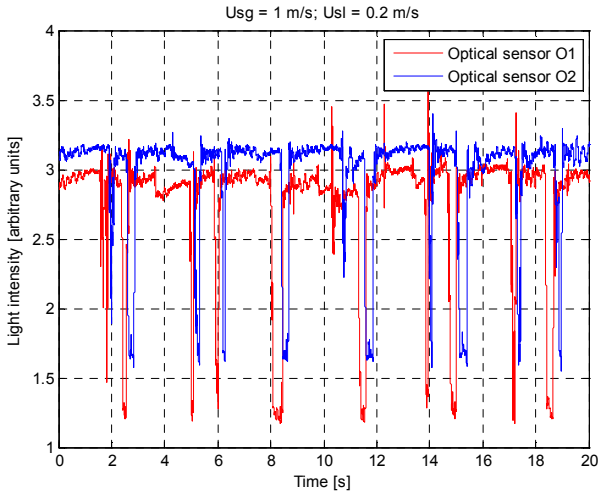

Figure 6: Optical signals at positions O1 (solid line), O2 (dashed line) as function of time for a flow of $u_{s,l}$=0.2 m/s; $u_{s,g}$=1.0 m/s.

The optical signal picture (Figure 6) shows the slugs passing by each sensor position. Slug velocity can be calculated by determining the time shift between peaks, indicating how long it took a slug to travel from one sensor to the next one. The slug frequency is determined based on a peak count, counting how many slug passed a sensor in a given time period. The slug length was determined in two ways: using the width of the peaks in the optical data and using the camera data.

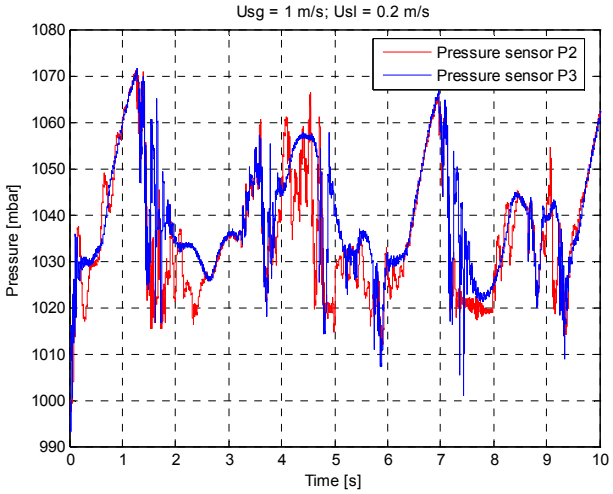

Figure 7: Pressure signals at position P2 and P3 as function of time for a flow of $u_{s,l}$=0.2 m/s; $u_{s,g}$=1.0 m/s.

The data from the transducers upstream of the bend were used to conduct a similar analysis based on pressure signals. The pressure data (Figure 7) show a trapezium profile, typical for the slug regime. This shape is due to the increased pressure drop in the tube from the outlet to the pressure measurement position due to the presence of the slug. The increasing slope is the time it takes for the liquid slug to flow past the measurement position (l_{slug} / u_{slug}). The length of the plateau corresponds to the time it takes the slug to flow from the pressure sensor position to the outlet.

In Figure 8, the slug velocity (u_{slug}) is compared to literature data. The Collins relation is used, which is given by [6]:

$$u_{slug} = C_0 u_m \tag{3}$$

with u_m the mixture velocity [m/s], which is the sum of the superficial gas and liquid velocity ($u_{s,g}$ + $u_{s,l}$) and C_0 the distribution parameter defined by:

$$\begin{aligned} C_0 &= 2 && \text{for } \mathrm{Re}_m < 2300 \\ C_0 &= \frac{\log(\mathrm{Re}_m)+0.089}{\log(\mathrm{Re}_m)-0.74} && \text{for } \mathrm{Re}_m > 2300 \end{aligned} \tag{4}$$

with the mixture Reynolds number (Re_m) defined by:

$$\mathrm{Re}_m = \frac{\rho_l u_m D}{\eta_l} \tag{5}$$

in which ρ_l the liquid density [kg/m^3], D the tube diameter [m] and η_l the liquid viscosity [Pa·s].

The experimentally measured slug velocity compares very well with the Collins relation, especially when well-defined slugs are present. The transitional cases are described less satisfactorily by this relation.

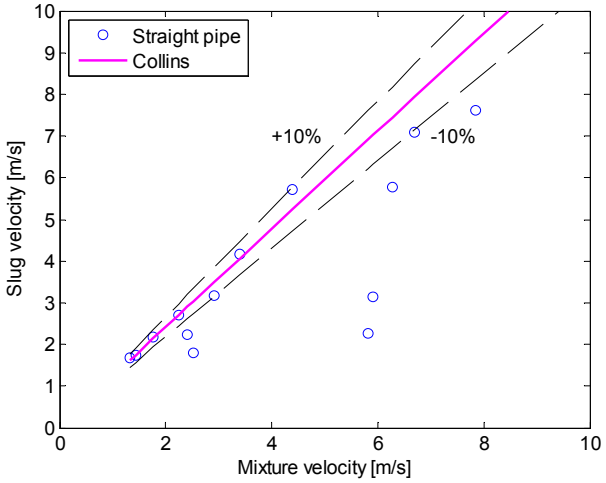

Figure 8: Slug velocity as function of mixture velocity.

The comparison with the classic models is also reasonable with respect to the slug frequency (f_{slug}). In Figure 9, the results are compared to a model by Fetter [7]. This model corresponds well with other classical models such as Manolis [8] and Heywood and Richardson [9]. This model gives the slug frequency as:

$$f_{slug} = 0.0175 \cdot \mathrm{Fr}_{\mathrm{Fet}}^{1.37} \tag{6}$$

with the Fetter slug frequency Froude number defined as:

$$Fr_{Fet} = \frac{u_{s,l}}{gD}\left(\frac{21.3+u_m^2}{u_m}\right) \tag{7}$$

The agreement is very good for the lower gas velocities. Similar to the slug velocity, for the higher gas velocities there is not a good agreement between the frequency measurements and the Fetter model. Instead of an increase, the frequency decreases. The reason for this behaviour could be that for the higher gas velocities the length of the tube is not large enough and the slugs are still accelerating and they are not yet fully developed. The frequency can also be expressed as a Strouhal number. The Strouhal number is defined as:

$$Sr = \frac{fD}{u_{sl}} \tag{8}$$

In Figure 10, the Strouhal number is plotted as function of the no-slip liquid hold-up for the current experiments and for literature data for different tube diameters. The current measurement results are in fair agreement with the other literature data.

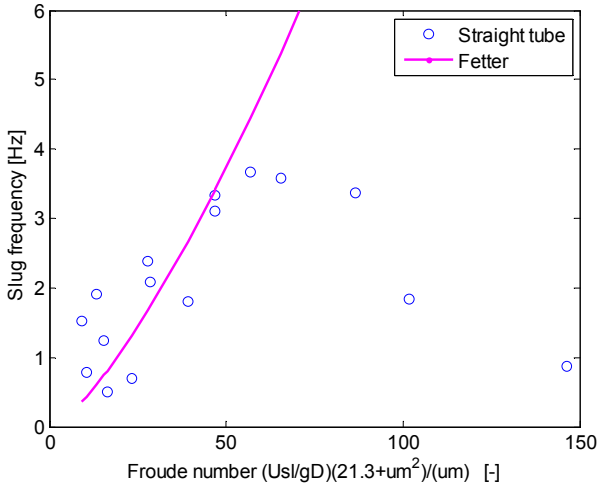

Figure 9: Slug frequency as function of Fetter slug Froude number.

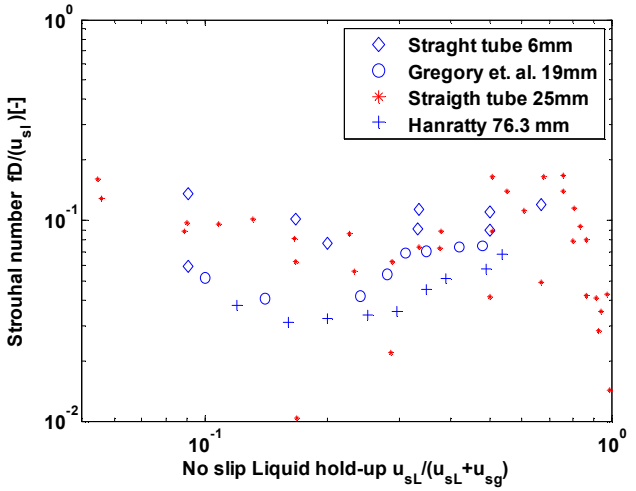

Figure 10: Strouhal number as function of no slip liquid hold-up. Comparison with results from Cargnelutti [3], Gregory and Hanratty [10].

Forces

As mentioned before, forces on pipes and bends in a multi-phase flow can be much larger than in a single-phase flow. Slug flow consists of masses of liquid (slugs) with the high density of the liquid phase, travelling at a high velocity dictated by the gas phase. In a straight section of pipe, the main excitation mechanism is turbulent noise and pressure change as a slug passes. In a bend, however, slug momentum changes in a relatively short time period, causing large forces. In a single phase flow the force on a bend is due to a change in pressure along the pipe and due to a change in momentum direction. In the case of a bend in slug flow, both can become very large, because both direction and fluid density to vary sharply.

Based on experiments on vertical U-bends with tubing size D = 20.6 mm, Riverin proposed a relation for the dimensionless force on a bend:

$$\overline{F_{rms}} = \frac{F_{rms}}{\rho_l u_m^2 A} = CWe^{-0.4} \tag{9}$$

with We the Weber number defined as

$$We = \rho_l u_m^2 D / \sigma \tag{10}$$

In his experiments Riverin found a good fit with a constant of C=10.

On Figure 11 an example of a typical force measurement in the frequency domain is plotted.

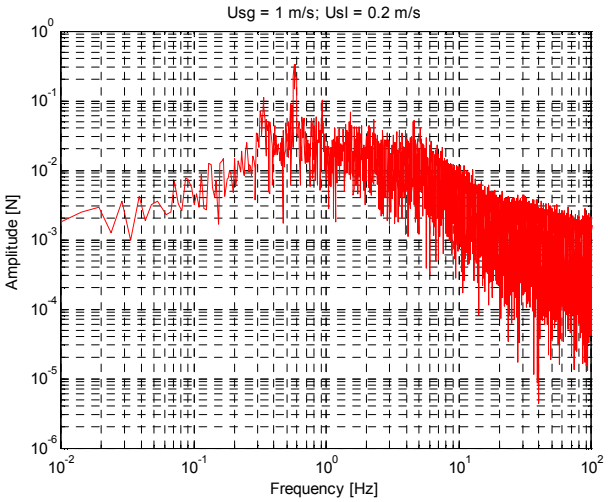

Figure 11: Frequency spectrum for a characteristic measurement.

In Figure 12, the experimental results are plotted as a function of the Weber number for the Bend1 configuration. A distinction in flow regime is made between single phase flow, slug flow, stratified flow and annular flow. A comparison of the forces generated in various flow regimes showed that the highest (relative) excitation forces are presented in the slug flow regime. The other extreme case is the annular flow regime, where the forces are the lowest. This is true for the relative forces. In Figure 13 the absolute values of the forces are plotted. In this figure it is clear that the forces generated by the annular flow regime are on the same order of magnitude as the forces generated by the slug flow, due to the much higher

absolute velocities associated with the annular flow. The forces generated in the stratified flow regime lie between these extremes. One of the main reasons for this is liquid content. Due to its high density, liquid carries much more momentum than gas travelling at similar velocities. Therefore, the momentum change in the bend is much larger for liquid than for gas. This can be properly seen in Figure 14, in which the dimensionless force is plotted as a function of the no-slip liquid hold-up. This is done for the four one inch geometries. As a comparison, measurement results of a scale of 6mm are included. For higher liquid loads the dimensionless force appears to asymptotically approach a limit of order 1. In a single phase flow, where a constant mass flow changes direction, the force can be derived from momentum change as:

$$F_R = \sqrt{2}\rho \cdot A \cdot U^2 \tag{11}$$

At high liquid load, the flow behaves as single phase. Therefore, the force approaches this limit. When both flow regimes are possible at the same no-slip liquid hold-up, the annular flow regime leads to lower forces. This is very likely due to the higher degree of mixing in the case of the annular flow due to droplet entrainment, and due to the fact that annular flow shows a more uniform liquid distribution in time. Momentum changes with time – and hence forces – are smaller. Rather than being located in relatively large mass concentrations, as occurs in slug flow, the liquid travels as a lower mass film along the tubing walls. This means the effective density of the two-phase flow travelling through the bend changes in a smaller degree, thus reducing momentum change. Therefore, the forces also decrease.

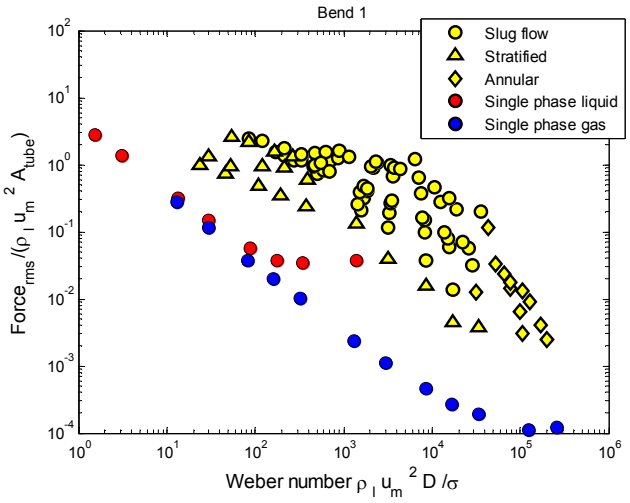

Figure 12: Dimensionless force as function of the Weber number. Red indicates single phase liquid, blue single phase gas, circles indicate slug flow, triangles stratified flow and diamonds annular flow.

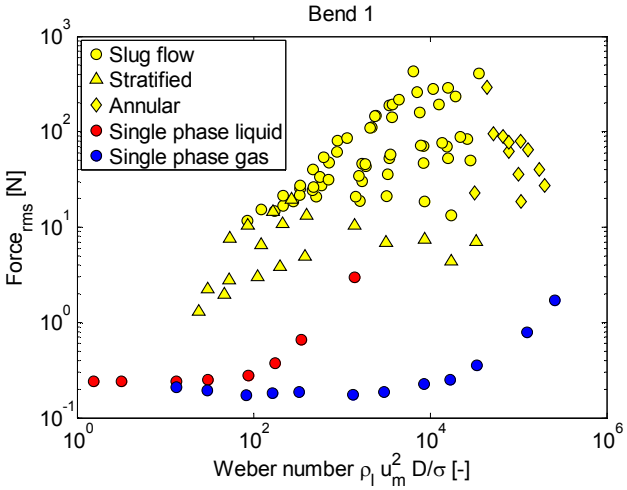

Figure 13: Absolute force as function of the Weber number. Red indicates single phase liquid, blue single phase gas, circles indicate slug flow, triangles stratified flow and diamonds annular flow.

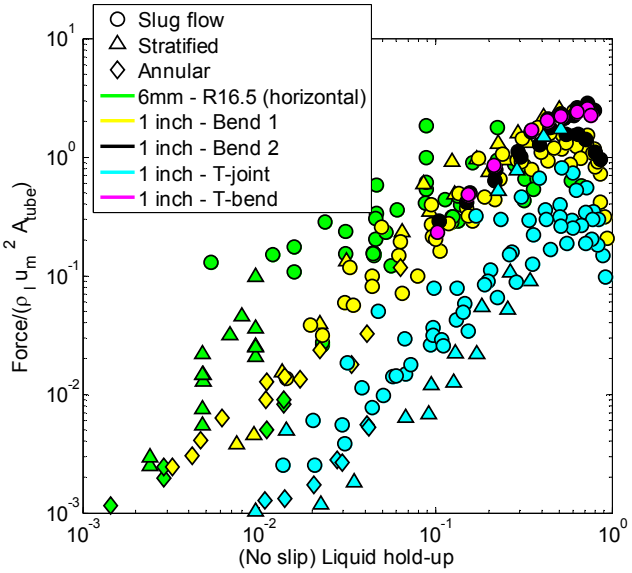

Figure 14: Dimensionless force as function of no-slip liquid hold-up. T-bend indicated the T-joint geometry with one leg closed off.

In Figure 15 the dimensionless force is plotted as function of all geometries. For comparison, results of measurements on a scale of 6 mm have been added as well as the the relationship proposed by Riverin. The relationship is plotted with different values for the constant C: C=10, as used by Riverin for his data set and C=3.51, which is the best fit with the slug flow experiments for the 6mm experiments. From this comparison several observations can be made:

- The results for Bend1 and Bend 2 are very comparable. This could be due to the fact that the slug length was typically larger than the bend radius.
- The results for the T-joint are lower than the Bend experiments. This can be explained from the fact that the flow is symmetrically splitted in two. This results in lower forces. The difference in axial and perpendicular forces for the Tjoint are plotted in Figure 16. The axial forces (sensor F2) are about twice the force in the perpendicular directin (sensor F1).
- The results for the T-bend are comparable to the Bend experiments. In practice the closed leg filled almost completely with liquid and a sharp bend is formed in that case.
- The forces in the 6 mm scale were slightly lower than for the 1 inch experiments. This was unexpected as the slugs in the 1 inch scale experiments contain more gas than for the smaller scale. The difference could be due to the stiffness of the material (glass vs. perspex).
- The current experiments show higher forces also compared to the Riverin experiments.

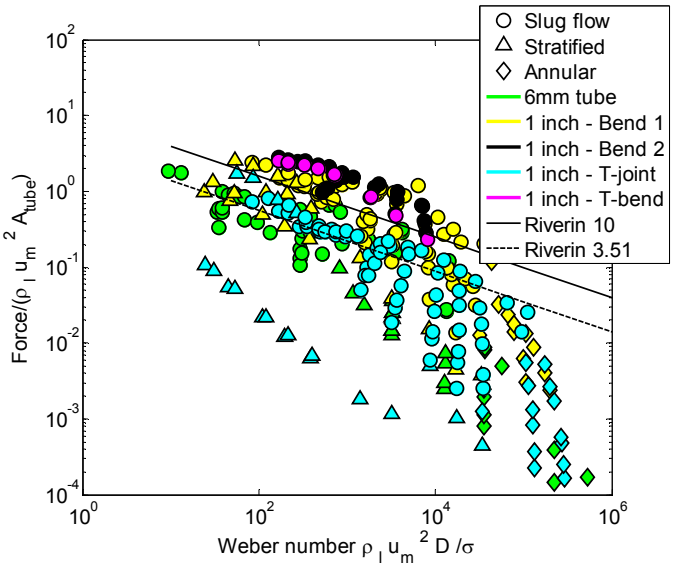

Figure 15: Dimensionless force as function of Weber number.

As discussed, in the T-joint the forces in the axial direction (sensor 2) are much higher than in the perpendicular direction (sensor F1). This is made clear in Figure 16. In this figure, the ratio of the measurements of force sensor 1 to force sensor 2 is plotted as function of the Weber number. This is done for all four geometries. For Bend1 and Bend2, the axial force is somewhat smaller than the perpendicular force. The ratio is about 2. This is likely due to the flexibility of the system. More movement is allowed in the perpendicular direction than the axial one. The rapid increase for the larger Weber number, for which the flow regime is annular/mist, is due to the very low forces on the bend. For the T-joint it is obvious that the axial force is larger than the perpendicular one. In the T-bend case, the forces in the perpendicular direction are three to five times as high as the axial ones. This could be caused by the imbalance in the T-joint because the closed end was full with liquid.

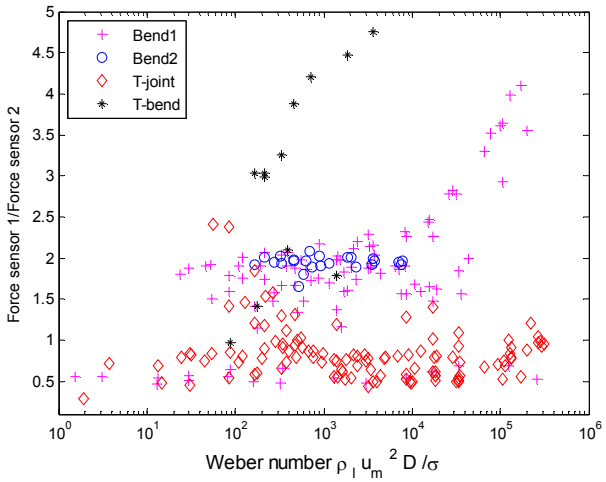

Figure 16: Ratio of force sensor 1 to sensor 2 as function of Weber number.

Model

A very simple model to predict the forces due to slug flow can be made by calculating the momentum change of a slug travelling through the bend. This results in the following expression for resultant force F_R:

$$F_R = \sqrt{2}\rho_l u_{slug}^2 A \tag{12}$$

in which we assume that the slug cross-sectional area is equal to the pipe cross-sectional area. Note that friction and gravity effects are not included in this simple model.

The part of a slug period where there is a slug moving through the bend is approximately equal to the liquid hold up (α_l). During the remainder of the period, we assumed the effective force on the bend to be zero. This means that the average force is given by:

$$F_{mean} = \alpha_l F_R \tag{13}$$

From this assumption, average values over a slug period can be calculated as:

$$F_{rms}^2 = F_{mean}^2 + F_{std}^2 \tag{14}$$

By definition:

$$F_{std}^2 = \alpha_l (F_R - F_{mean})^2 + (1-\alpha_l)(0 - F_{mean})^2 \tag{15}$$

Then,

$$F_{rms}^2 = (\alpha_l F_R)^2 + \alpha_l (F_R - \alpha_l F_R)^2 + (1-\alpha_l)(0-\alpha_l F_R)^2 \tag{16}$$

No random excitation due to turbulence is taken into account is this simple model, which is only based on momentum change. In Figure 17 a comparison is made between the simple model results (slug model in the figure) and the measurements. In the slug flow regime, the comparison is acceptable. However, this model fails for the annular flow and stratified flow regimes. In these regimes, there are no distinct slugs of liquid travelling along the tube. Then, for these flow regimes the forces can be estimated by simply taking the mixture momentum (mixture model in Figure 17):

$$F_R \approx \sqrt{2}\left(\rho_m u_m^2\right)A \tag{17}$$

This is analogous to the single phase situation, where a constant mass flow of fluid is changing direction. The flow is treated as if it were single-phase, defined by a mixture density and velocity.

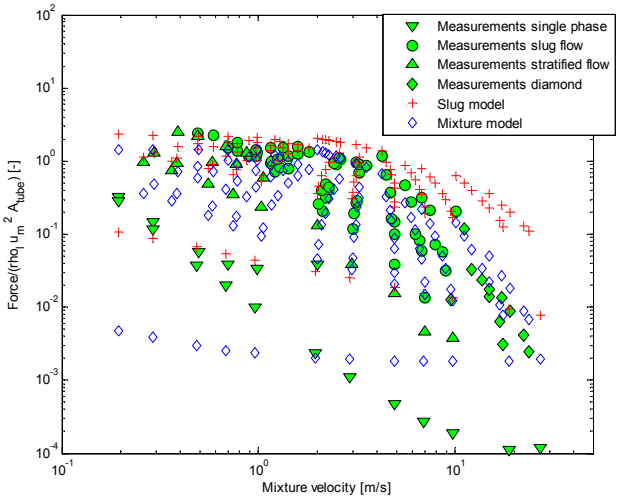

Figure 17: Dimensionless force as function of mixture velocity.

The single phase experiments could not be described well with this approach, neither for the single phase gas or the single phase liquid. The primary reason is of course that turbulence is not taken into account in the simple estimation.

CONCLUSIONS

The flow characteristics of an air-water flow through 1 inch tubes have been analyzed. The flow regime map corresponds well with the classic flow maps. This confirms the validity of the experimental set-up. The slug velocity model describes the experiments well as long as the slug flow is well defined. It fails close to the boundary between the slug flow and annular flow regime. The slug frequency model works well for low gas velocities but fails to describe the results at higher gas velocities.

Measured forces vary significantly depending on flow regime. The highest force levels are observed in the slug flow regime, whereas annular flow gives the lowest force levels. The forces decrease roughly linearly with the liquid content. The force amplitude was measured to be between 1 and 10 times the liquid momentum based on the mixture velocity. A comparison showed higher force values that those reported by Riverin.

No effect of bend radius was found. Three bends were measured (a sharp edged bend, a large bend radius bend and a bend with a closed side branch), and all results were comparable. The results for a real T-joint were significantly lower than for the bends.

In case of slug flow, the measured results can be described assuming a simple slug unit model. In annular and stratified flow a different model is required, since no slug unit is present. Instead, excitation force can be estimated using mixture properties. This mixture approach also describes the forces for the slug regime relatively well. Only the single phase flow is not described properly with this mixture model, as would be expected.

ACKNOWLEDGMENTS

The authors are grateful that the ISAPP consortium (Shell, Delft Technical University, TNO) allowed the publication of this work.

REFERENCES

[1] Riverin, J.L., De Langre, E., Pettigrew, M.J., 2006, "Fluctuating forces caused by internal two-phase flow on bends and tees", JSV 298, pp. 1088-1098.

[2] Tay, B.L. and Thorpe, R.B., 2004, "Effects of Liquid Physical Properties on the Forces Acting on a Pipe Bend in Gas–Liquid Slug Flow", Chemical Engineering Research and Design, 82(3), pp. 344-356.

[3] Cargnelutti M.F., e.a, 'Two-phase flow-induced forces on bends in small scale tubes', PVP2009-77708, ASME PVP conference Prague, 2009

[4] Mandhane, J.M., Gregory, G.A., and Aziz, K., 1974, "A Flow Pattern Map for Gas-Liquid Flow in Horizontal Pipes", Int. J. Multiphase Flow, 1(4), pp. 537-553.

[5] Chiaasiaan S.M. , 'Two-phase Flow, boiling, and condensation'(1st edition, 2008)

[6] Collins, R., de Moraes, F.F., Davison, J.F. and Harrison, D., 1978, "The motion of a large gas bubble rising through liquid flowing in a tube", J. Fluid Mech., 89, pp. 497-514.

[7] Fetter, C.P., 1988, "Development of a Clamp-on Acoustic Two-Phase Flow Meter", M.Sc. thesis, TUDelft, Netherlands.

[8] Manolis, I.G., 1995, "High pressure gas–liquid slug flow", Ph.D. Thesis, Imperial College, London, UK.

[9] Heywood, N.I. and Richardson, J.F., 1979, "Slug flow of air–water mixtures in a horizontal pipe: Determination of liquid hold-up by γ-ray absorption", Chem. Eng. Sci. **34**, pp. 17–30.

[10] Woods, B.D., Fan, Z., Hanratty, T.J., 2006, "Frequency and development of slugs in a horizontal pipe at large liquid flows", IJMP, 32(8), pp. 902-925.